Evaluating Tree Detection and Segmentation Routines on Very High Resolution UAV LiDAR Data

Luke Wallace, Arko Lucieer, and Christopher S. Watson

***Abstract*—Light detection and Ranging (LiDAR) is becoming an increasingly used tool to support decision-making processes within forest operations. Area-based methods that derive information on the condition of a forest based on the distribution of points within the canopy have been proven to produce reliable and consistent results. Individual tree-based methods, however, are not yet used operationally in the industry. This is due to problems in detecting and delineating individual trees under varying forest conditions resulting in an underestimation of the stem count and biases toward larger trees. The aim of this paper is to use high-resolution LiDAR data captured from a small multirotor unmanned aerial vehicle platform to determine the influence of the detection algorithm and point density on the accuracy of tree detection and delineation. The study was conducted in a four-year-old *Eucalyptus globulus* stand representing an important stage of growth for forest management decision-making process. Five different tree detection routines were implemented, which delineate trees directly from the point cloud, voxel space, and the canopy height model (CHM). The results suggest that both algorithm and point density are important considerations in the accuracy of the detection and delineation of individual trees. The best performing method that utilized both the CHM and the original point cloud was able to correctly detect 98% of the trees in the study area. Increases in point density (from 5 to 50 points/m^2) lead to significant improvements (of up to 8%) in the rate of omission for algorithms that made use of the high density of the data.**

***Index Terms*—Forestry, lasers, remote sensing, remotely piloted aircraft.**

I. Introduction

SUSTAINABLE forest management and decision-making processes require timely and accurate forest information. The information derived from airborne LiDAR point clouds is increasingly used to support decision-making processes within everyday forest operations. A number of the processes and algorithms used to derive information from LiDAR have reached maturity, and it can now be considered a standard data source for defining the spatial characteristics of a managed forest [1], [2].

Manuscript received January 15, 2013; revised July 10, 2013, November 6, 2013, and February 4, 2014; accepted March 23, 2014.

The authors are with the School of Land and Food, University of Tasmania, Hobart, Tas. 7001, Australia (e-mail: Luke.Wallace@utas.edu.au; Arko.Lucieer@utas.edu.au).

Color versions of one or more of the figures in this paper are available online at http://ieeexplore.ieee.org.

Digital Object Identifier 10.1109/TGRS.2014.2315649

Forest inventories are able to be derived from LiDAR data using one of two approaches. The area-based approach, first reported in Nelson *et al.* [3], infers forest properties for an area of interest based on the relationship between field measurements and the empirical above-ground height distribution of canopy returns [4]. This approach is used to estimate a variety of forest inventory attributes with high accuracy, including biomass, stand volume, and basal area [5]–[7]. To achieve this, however, extensive field sampling is required for model calibration and validation purposes [8]. The individual tree detection approach, first reported in Hyyppä and Inkinen [9], segments points representing each tree to determine individual tree properties such as position, height, canopy shape, and species.

The timing of silvicultural activities such as pruning, thinning, and harvesting is of crucial importance to the management of plantation forests. Due to the high costs of airborne surveys, the inventory information derived from LiDAR data is not often timed to coincide with these key growth stages. As such, decisions made based on these surveys often require input from alternate sources, such as growth models or field inventories, to be accurate. Mini-unmanned aerial vehicles (UAVs) have been recently proposed as an alternative platform for the capture of LiDAR data [10], [11]. UAVs have been shown to allow very high spatial resolution data (50 to 120 pulses per square meter (p/m^2)) to be captured rapidly and on demand.

Data from a mini-UAV are captured without significant occlusion of the top of the canopy and therefore has similar characteristics to full-scale airborne data [12]. The high-density data collected from UAV platforms have the potential to replace the use of laborious and costly field sampling, which is still commonly performed in direct support of silvicultural treatments and decision-making processes. Nevertheless, the low-altitude flight and minimal flight time restrict the area that can be captured in a single flight. This suggests that in order to take full advantage of the unique combination of high spatial data collected at low deployment costs, accurate and robust delineation of individual trees is essential in order for UAVs to be considered a viable and practical tool within the forest industry.

Several algorithms have been developed to delineate trees from LiDAR point clouds [13]–[18]. The majority of these algorithms aim to exploit the fact that tree tops represent the highest part of the landscape and therefore attribute local maxima within the data to individual tree tops. This is followed by the segmentation of feature space to produce representations

TABLE I
PROPERTIES OF THE SIX PLOTS FOR WHICH FIELD DATA WERE COLLECTED WITHIN THE *Eucalyptus Globulus* PLANTATION

Plot	Stem Count	Min Height (m)	Max Height (m)	Mean Height (m)	Mean DBH (m)	Mean Crown Width (m)	Mean Pulse Density (p/m^2)
1	49	2.6	8.7	5.71	0.07	3.01	67
2	34	3.0	8.1	6.47	0.09	3.79	163
3	59	5.9	10.9	8.93	0.09	3.60	65
4	78	3.1	9.8	7.05	0.08	3.17	68
5	46	5.8	10.2	8.80	0.09	3.07	61
6	42	6.8	10.5	8.86	0.11	3.05	87

of trees, for example, using region growing [19]. Differences between these algorithms typically relate to the amount of smoothing applied to the data to remove false maxima, postprocessing of the results (e.g., data smoothing), or the feature space in which the segmentation is employed. For instance, detection and segmentation processes have been performed directly on a point cloud feature space [20]–[22] or on a feature space, which have been derived from the initial point cloud, such as a canopy height model (CHM) [23] or voxel space [24].

Difficulties in detecting and delineating individual trees often produce an underestimation of the number of stems and a bias toward larger trees or those in the top tier of multilayered forests [25]. The under- or overdetection of stems has been shown to have a significant effect on the accuracy of inventory estimates derived from these approaches [26]. The extent of this effect is dependent on the accuracy of the reported algorithms, which significantly varies; Pitkänen *et al.* [27], for instance, achieved a tree delineation accuracy value of only 40% in comparison with Heinzel *et al.* [28] who achieved accuracy values of up to 88%. Directly comparing these results, however, could be misleading due to different data set properties (i.e., pulse density and number of returns per pulse) and forest conditions (stem density for instance).

In order to provide an objective estimate of the accuracy of different routines, several studies comparing the application of these routines under varying conditions have been completed [29]–[32]. Kaartinen *et al.* [32] for example, compared 13 different algorithms under boreal forest conditions concluding that the main factor affecting the accuracy of the tree detection and delineation was the algorithm employed. Whereas, Vauhkonen *et al.* [30] compared six different algorithms across varying forest structures and suggested that accurate delineation of trees is highly dependent on the properties of the forest, including stand density and the spatial pattern of the trees.

The focus of these comparative studies, as well as the development of most algorithms, has primarily been the delineation of individual trees from LiDAR data sets of typical densities captured for forest inventory purposes (from 1 to 10 p/m^2). Higher point density data have been shown to improve the measurement of plot level statistics [33], and it has been hypothesized that higher density data, such as those obtained by UAV platforms, are likely to provide a better representation of the features used to delineate trees and therefore improve the accuracy of these methods [15].

The aim of this paper is to apply and assess the ability of tree detection algorithms to detect and delineate individual trees within a single-stage four-year-old *Eucalyptus globulus* plantation using high-density UAV LiDAR data. This paper evaluates the effect of point density on the accuracy of tree detection and delineation using several tree detection algorithms with tree count, tree location, and crown width used to inform the accuracy of the results. A UAV platform is used to collect on-demand high-density data, which is subsequently decimated to providing a comparison to densities collected with modern full-scale systems. The results from each approach and at each density are subsequently validated against data acquired from field surveys.

II. STUDY AREA AND DATA COLLECTION

The study was conducted in a four-year-old *Eucalyptus globulus* plantation located in Southern Tasmania, Australia (E146° 56′ 54″, S43 ° 05′ 18″). Trees within the coupe were planted at 3-m intervals along rows 3 m apart. A field survey of individual trees within six plots with fixed radii of 12.62 m was conducted. Within each plot, we recorded the position, the crown diameter, the tree height, the number of overlapping crowns, and the presence of forks and ramicorns for each plantation species. For non-plantation species (representing 2% of the recorded trees), only position of the stem at breast height and height were recorded. Plot centers were surveyed using a differential GPS receiver (0.05-m accuracy), and stem heights and locations were measured using a forestor vertex hypsometer and compass bearing to the plot center (giving an approximate 1.0-m accuracy). Crown diameter was measured as the mean of the largest diameter branch and the diameter of a branch at 90° to this initial measurement. Summary statistics of the field data collected within the six plots are given in Table I. The stem densities of the plot ranged from 680 to 1560 stems/ha suggesting inconsistent planting and some loss of trees.

Discrete return LiDAR data were collected over each plot with the TerraLuma UAV-LiDAR system described in Wallace *et al.* [11]. An Ibeo LUX laser scanner, which measures up to 3 returns per pulse, was mounted on the UAV and used to collect observations within a scan angle range of $+/-30°$. Two perpendicular passes were flown over each plot at an approximate flying height of 40 m above ground level (AGL) (and 32-m above-mean crown height). The point clouds from the perpendicular flights were merged resulting in final point clouds with point densities of at least 60 p/m^2 covering each plot with an 8-m buffer (Table I). For the purpose of independent validation of horizontal and vertical accuracy, six reflective targets were placed under each flight path and surveyed with Real-Time Kinematic GPS. The locations of these targets within the generated point clouds suggested that root-mean-square errors (RMSEs) of better than 0.17 m horizontally and

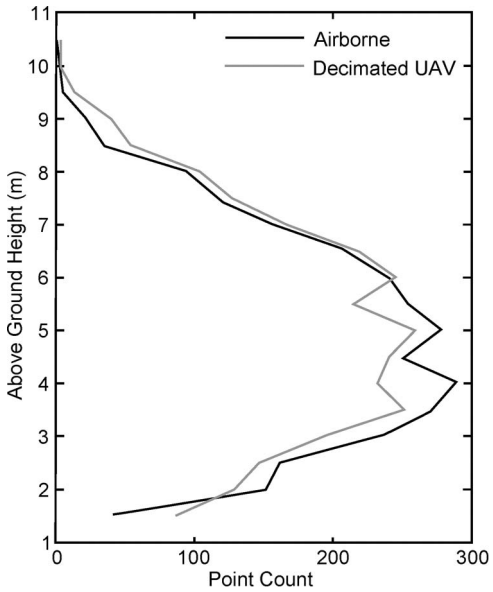

Fig. 1. Above ground height distributions of full-scale airborne and UAV data decimated to the same density (8 p/m^2) captured over a coincident area.

0.11 m vertically were achieved (consistent with Wallace *et al.* [11]). The resultant point clouds were clipped to include a 5-m buffer around the plot area to minimize edge effects in the tree detection and delineation algorithms.

III. Materials and Methods

A. Point Cloud Preprocessing

In order to determine any improvement provided by the use of high-density UAV data, the full density point cloud was decimated to produce four further point clouds with densities of 2,5, 10, 25, and 50 p/m^2 to simulate data collected at different densities. The decimation procedure follows Vauhkonen *et al.* [34], which involves selecting an individual pulse from each cell within a grid, with a cell size set to match the desired point density. In this case, a random starting point and orientation were selected for each grid, and a random pulse selection was made from the pulses that fell within each cell. Every return from each selected pulse was included in the decimated point cloud. This methodology was preferred over techniques that remove points based on scan lines (i.e., Raber *et al.* [35]) as it produces a homogeneous point density and a similar above ground height distribution of canopy returns to full-scale LiDAR data (see Fig. 1). This allows the decimated data to be used as a proxy for full-scale data.

In order to obtain forest information from a LiDAR point cloud, initial processing requires the extraction of all ground points. This includes the computation of point height AGL. There are numerous algorithms available to distinguish bare ground points from vegetation and other above ground points (e.g., see review in Meng *et al.* [36]). In this paper, we applied the iterative filtering and thresholding algorithm developed by Axelsson [37]. The approach uses a progressive triangular irregular network (TIN) densification method where new points are iteratively added to a TIN model of ground points if they are within defined angle and distance thresholds. The ground points identified by this algorithm were then used to create a 0.1-m-resolution digital terrain model using natural neighbor interpolation. The above ground height of all nonground points was then calculated using this surface resulting in a normalized point cloud. This approach was applied to the full and decimated point clouds independently with initial threshold angles set (to between 5° and 9°) for each decision rule to achieve optimum results at each point density.

The normalized point clouds were then used to generate CHMs by assigning each pixel with the maximum height of all the points that fall within its boundaries. Missing data and sinks (the result of pulses that have penetrated the canopy) were replaced using a pit-filling algorithm outlined in Ben-Arie *et al.* [38] in which pits are identified and replaced by the median value of the eight surrounding cells. The cell size of the generated CHM is dependent on the individual tree detection algorithm used, as discussed in the following section.

B. Individual Tree Detection Algorithms

The tree detection and delineation algorithms evaluated in this paper were selected to be representative of the three different feature spaces often used in the literature: 1) the original 3-D point cloud space; 2) voxel space; and 3) the CHM (as depicted in Fig. 2). One algorithm from each feature space and one hybrid algorithm have been evaluated in this paper. These algorithms have been selected as they are commonly used in the literature, and comparative studies such as Kaartinen *et al.* [32] and Vauhkonen *et al.* [30] have indicated that the tree detection accuracy values are relatively high. Where necessary, the following algorithms have been adapted to ensure that the increased resolution of the data is fully utilized and to account for the properties of the tree crowns found in the study area.

PDD: Several algorithms that delineate trees directly from the point cloud have been presented within the literature [16], [17], [21]. The algorithm employed here is an adaption of the technique outlined in Li and Guo [21]. The approach aims to exploit the changes in relative space between individual trees at different heights to determine a tree boundary. Beginning with the highest point in the normalized point cloud as the first tree, all other points are evaluated against a set of criteria to determine if they belong to this current tree. These are the two criteria.

1) If the point is not a local maxima within a given search radius (i.e., 2 m), it belongs to the current tree if the point is closer to a point within the current tree than any point already classified as a non-tree point.
2) If the point is a local maxima, the point belongs to a tree if it is within a 2-D distance (dt) of all points in the current tree and it satisfies criterion 1.

Once a tree has been segmented, the algorithm continues with the next highest unclassified point within the data set as a new tree. The search radius can be chosen arbitrarily; however, the threshold distance (dt) needs to be tuned to the structure of the forest being analyzed. In this case, two values (1.5 and 0.9 m) were used depending if the point being examined was above or below 5 m in normalized height. In Li and Guo [21],

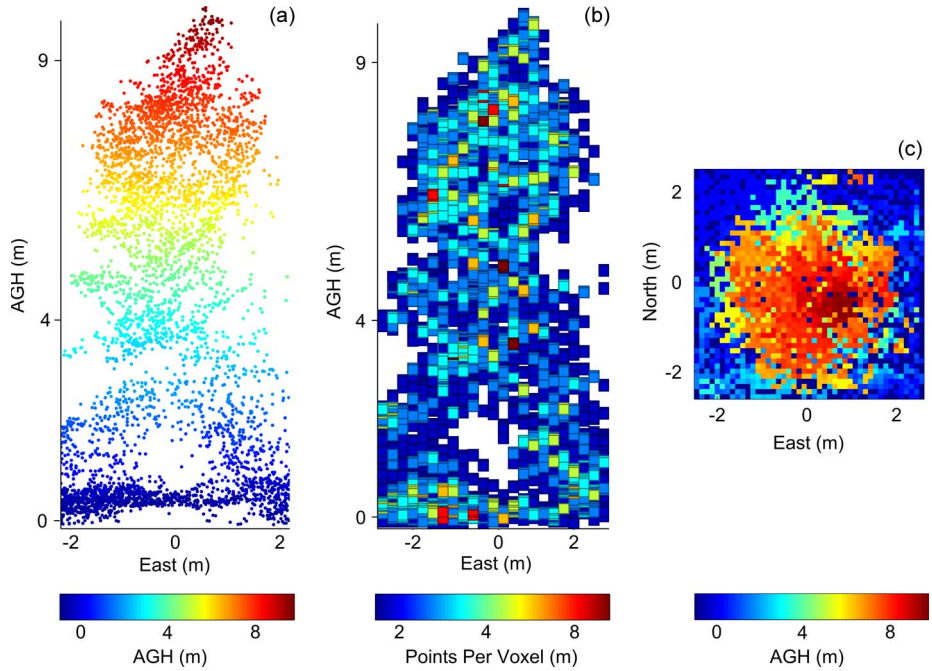

Fig. 2. Representation of the three feature spaces: (a) the original point cloud; (b) 0.2-m cubic voxel space; and (c) a 0.1-m-resolution CHM, analyzed in this paper as derived from an unfiltered point cloud.

the process is repeated until all points have been attached to an individual tree segment. However, due to the complexity of the understory and the large number of points in this paper, the search was stopped once all points 1.3-m AGL had been classified. This allows trees that have canopies extending to the ground to be almost completely delineated while stopping understory vegetation being recorded as belonging to a tree.

The algorithm presented by Li and Guo [21] is also extended by applying a further step to merge or split a tree depending on the crown radius of a segmented tree. For segments that are deemed potentially too large based on an area-to-height ratio, the algorithm is repeated with relaxed distance criteria. Segments that are too small to be a tree are merged with neighboring segments based on Euclidean distances. Tree location is taken at the location of the highest point within a segment, and crown width is determined based on the average distance of the furthest point from the tree location and the furthest point at 90° from this location.

VDD: The voxel space detection and delineation (VDD) algorithm is based on the algorithm outlined by Wang *et al.* [15]. The point cloud data are first projected into voxel space, where each voxel is attributed with the number of points it contains. Crown objects were defined in each horizontal voxel layer based on a hierarchal morphological algorithm, in which pixels with higher densities are assumed to be the most likely location of a tree crown [15]. The crown objects are traced through the voxel layers and merged if the intersection area of a segment in one vertical layer and the layer directly below is greater than 80% of both individual segment areas. In this paper, a higher resolution voxel space was employed, in comparison to Wang *et al.* [15], allowing the extra information in the UAV point cloud to be exploited. Three-dimensional tree location was defined as the center of the maximum voxel in which the tree occurred and crown width as the mean distance from this point to all boundary voxels of the horizontal projection of the tree from all merged layers.

CDD: The most common form of algorithm used to detect and delineate trees from LiDAR data is based on detecting local maxima within the CHM. The algorithms often first apply a smoothing strategy to eliminate any spurious maxima and minor tree level fluctuations caused by branches. The degree of smoothing is often determined based on the knowledge of the crown size to tree height [17] or by applying multiple filters and evaluating the results [39]. As the study area in this paper is a plantation, it is a reasonable assumption that the trees will all be approximately the same height and width. For this reason, a Gaussian filter with a 1.5-m kernel was applied and the degree of smoothing was varied depending on the point density and cell size of the CHM. Two different CHMs, i.e., a 0.50-m-resolution CHM detection and delineation (CDD_{50}) and a CHM with an optimized resolution to achieve an average of 2 pulses per grid cell $(\mathrm{CDD}_{\mathrm{opt}})$, were generated for each point cloud in this paper.

Local maxima were then derived from the smoothed surface using a 3×3 kernel and any maxima greater than 2 m were considered to be the location of a tree. Delineation of tree crowns was performed using marker-controlled inverse watershed segmentation with the local maxima found in the previous step as control markers [40]. The center of the cell containing the local maxima was considered as the tree location. The crown width of a tree was considered equal to the mean distance of tree location to the boundary of the segmented area as calculated in eight equally spaced directions. The initial direction was chosen to represent the largest possible value.

CDPD: A hybrid algorithm presented in the literature for delineation of trees within point cloud feature space is based on seeded k-means clustering [20], [41]. In this approach, local maxima were first identified from a smoothed (0.2-m

resolution) CHM with a similar smoothing strategy to the CDD algorithm applied. These maxima were used as seeds within the k-means clustering algorithm on a point cloud with a downscaled z-dimension by a factor of 1.5. Downscaling was performed such that tree objects appeared as spheres in the resultant point cloud. The scaling factor was chosen based on a general relationship between tree height and crown width [20]. The resulting cluster centers are used as tree locations. Crown width was then estimated as the mean of the radii from the tree location to all points forming the edges of the convex hull of the cluster.

C. Algorithm Tuning

Tuning of the input variables was carried out to ensure that each algorithm performed optimally for the forest type. The tuning procedure involved manually finding the parameters that optimized the omission and commission results of plot 5. This process was applied separately at each individual point density. As plot 5 was used in tuning the algorithms, it is not included in the tree detection results.

The search radius and two values of dt for the point cloud detection and delineation (PDD) algorithm were found to be constant across all point densities and related to the size of the crown. Similarly, the kernel size of (CDD_{50}), $(\mathrm{CDD}_{\mathrm{opt}})$, and CHM detection and point cloud delineation (CDPD) algorithms was found to be optimal at 1.5 m. The degree of smoothing was found to decrease from 2.8 to 1.6 with increasing point density. The optimal voxel width and depth used in the VDD algorithm were also found to decrease with increased point density. Voxel width was found to vary between 0.2 and 0.8 m, and thickness varied from 0.5 to 2.0 m.

D. Performance Evaluation

The performance of each tree detection algorithm was evaluated by applying the following procedure. Segmented trees were first linked to field-measured trees if the two crown areas overlapped by more than 20%. If the crown of more than one segmented tree overlapped a field-measured tree, the closest tree (based on 2-D Euclidean distance) was selected as a match. The unmatched trees within the field and LiDAR data sets were assigned as false negatives and false positives, respectively. The detection rate (estimated tree count in proportion to the number of field-measured tree count), omission errors (number of false negatives in proportion to field-measured tree count), and commission errors (number of false positives in proportion to the total number of predicted positives) were then determined for each algorithm and grouped based on field-measured height and if the tree was isolated or belonged to a group.

Stem location and crown width were used to provide an indication of the success of each algorithm in correctly delineating crown boundaries. Crown width was preferred over other metrics such as crown cross-sectional area or crown volume due to it being a more readily assessable field measurement and given the proven use of crown width in predicting inventory metrics such as diameter breast height [42]. The accuracy of these metrics was evaluated based on a comparison of the correctly matched trees with the collected field data. For crown width, the RMSE and bias were calculated as follows:

$$\mathrm{RMSE} = \sqrt{\frac{\sum_{i=1}^{n}(x_{nL} - x_{nF})^2}{n}} \tag{1}$$

$$\mathrm{Bias} = \frac{\sum_{i=1}^{n}(x_{nL} - x_{nF})}{n} \tag{2}$$

where x_{nL} and x_{nF} are the LiDAR and field measurements of each variable, respectively. Only correctly matched trees were used in these calculations; therefore, n is the count of correctly matched trees. RMSE and standard deviation were calculated for tree locations based on the difference between field and LiDAR measured locations.

TABLE II
OMISSION ERRORS (IN PERCENTAGE) FOR EACH TREE DETECTION CLASS WITHIN HEIGHT AND GROUPING CLASSES FROM THE FULL DENSITY DATA. A GROUP IS DEFINED AS TWO OR MORE OVERLAPPING CROWNS

Algorithm	Total (%)	2 to 5 m		5 to 10 m		> 10 m	
		Isolated (%)	Group (%)	Isolated (%)	Group (%)	Isolated (%)	Group (%)
PDD	6	11	20	3	8	0	8
VDD	8	11	40	3	10	0	8
CDD_{50}	9	6	50	5	10	10	0
CDD_{OPT}	4	6	20	2	8	0	8
CDPD	5	6	40	3	5	0	0
Tree Count		20	11	117	99	12	13

IV. RESULTS

A. Tree Detection

All five of the implemented algorithms were detected over 90% of the stems using full density data. For these point clouds, the number of trees found by the algorithms corresponded to between 99% (VDD) and 107% (PDD) of the field-measured trees. The percentage of field-measured trees correctly linked to LiDAR delineated trees was between 92% (CDD_{50}) and 97% $(\mathrm{CDD}_{\mathrm{opt}})$. In all algorithms, small trees, which occurred in groups, had the highest rate of omission (Table II). The small number of trees (11) of this type within the plots therefore inflated the overall detection rate. The $\mathrm{CDD}_{\mathrm{opt}}$ and the PDD algorithms omitted only 20% of trees in this class; however, the PDD algorithm also omitted 11% of the small isolated trees. At full density, commission errors for most algorithms typically involved the oversegmentation of large trees or trees that were forked or presented a large ramicorn. However, the PDD algorithms also tended to oversegment low branches into trees. Thus, the PDD algorithm had the highest rate of commission (14%), whereas the other algorithms had commission rates between 5% (CDPD) and 8% (CDD_{50}).

Commission errors typically increased for sparse stands, for example, plot 6, which contained the fewest stems had above average commission errors for all algorithms. Plot 2 had an average stem count of 52 stems/ha and had the lowest omission rate of all algorithms, with only one tree being omitted. Plot 4 had the highest stem density and typically gave results similar to other plots for all algorithms apart from CDD_{50}, which gave a commission rate double that of any other algorithm in this plot.

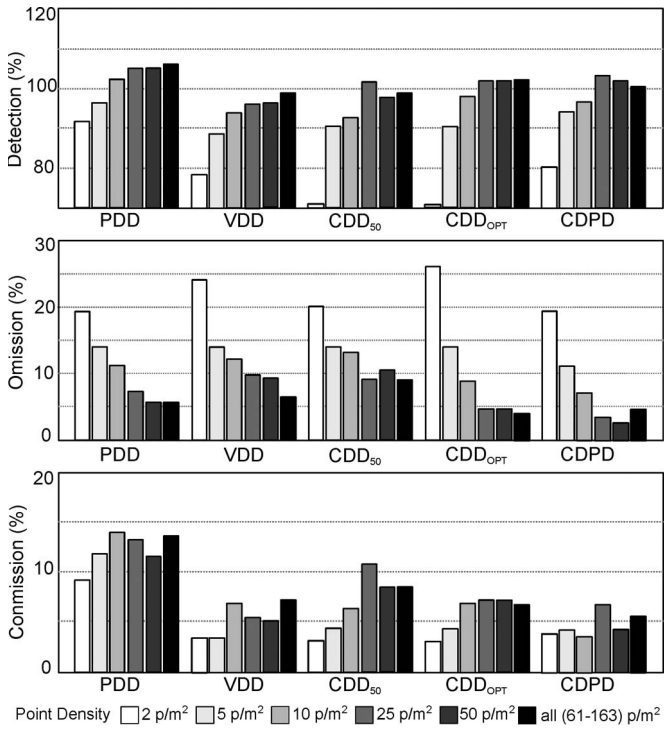

Fig. 3. Detection, omission, and commission rates for the five algorithms utilizing the five different point densities. There was a total of 272 trees within 5 plots.

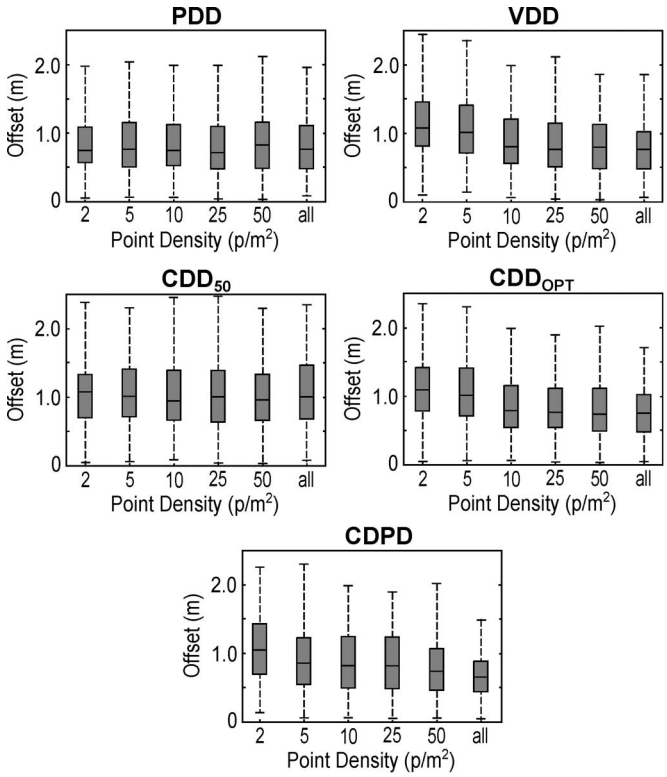

Fig. 4. Box plot (showing the 5th, 25th, 50th, 75th, and 95th quartiles) showing the absolute offsets between field and LiDAR measured tree locations for each algorithm and at each density.

At 2 p/m^2, all algorithms showed high rates of omission (up to 26%) resulting in a low detection rate. Significant reductions in the omission rate were seen when the point density was increased to 5 p/m^2 (see Fig. 3). Further increases in point density from 5 to 50 p/m^2 allowed for improved tree detection accuracy across every algorithm apart from CDD_{50} (see Fig. 3). For this algorithm, the tree detection results were best at 25 p/m^2 when 101% of trees were detected; however, the commission and omission errors were lower in the full density data and 5 p/m^2, respectively.

The result of decimating the point cloud for all other algorithms was an increase in the omission error. This is best demonstrated by the PDD algorithm, which, at 5 p/m^2, had high omission (14%) and commission (10%) errors. At 50 p/m^2, the omission rate decreased to 5% and the commission error remained similar at 12%.

Improvement between the 50-p/m^2 point clouds and the full density point clouds was seen in the $\mathrm{CDD}_{\mathrm{opt}}$ algorithm. The omission and commission rates marginally increased for both the PDD and CDPD algorithms between the 50-p/m^2 and full density point clouds. Furthermore, similar detection results were found for plot 2 when using a point cloud decimated to 100 p/m^2 in these two algorithms. For instance, in the CDPD algorithm, the detection rate was 106% (omission 0% and commission 6%) at 50 p/m^2, 105% (omission 0% and commission 5%) at 100 p/m^2, and 107% (omission 0% and commission 7%) at full density.

B. Tree Location

For each tree matched to an equivalent field-measured tree, the difference in the field and LiDAR measured locations was typically within the expected accuracy of the field data for each algorithm (see Fig. 4). This difference was similar across four of the five algorithms when using full density data, as indicated by the RMSE of 0.90 m for the CDPD, 0.94 m for $\mathrm{CDD}_{\mathrm{opt}}$, and 0.98 m for VDD and PDD. The CDD_{50} algorithm had the highest RMSE at full density (1.25 m), which is a result of data resolution as tree location was taken at the center of a 0.5-m cell. This also meant that for this algorithm, increased point density had no significant effect on the accuracy of tree locations (see Fig. 4). The $\mathrm{CDD}_{\mathrm{opt}}$, VDD, and CDPD algorithms showed significant improvement with increasing point density (up to 0.28 m in the $\mathrm{CDD}_{\mathrm{opt}}$ algorithm).

Differences in the field and LiDAR measured tree location typically increased within dense stands and for stems further from the plot center. These increased differences are a function of the increased error in the field measurements as opposed to the accuracy of the detection algorithms. Furthermore, trees in the densest plot (plot 4 with 79 stems) had the highest RMSEs in all algorithms (for instance, 1.02 m in the CDPD algorithm).

Fig. 5 shows that for each tree, the LiDAR measured locations found in each algorithm have similar offsets (both in magnitude and direction) from the field-measured location. This consistent error is due to the comparison of relatively inaccurate stem locations measured in the field with tree top locations measured from the LiDAR data in all but the CDPD algorithm, which used cluster centroids to derive stem locations. The difference in field and LiDAR measured tree location when using the lower density point clouds was more variable between

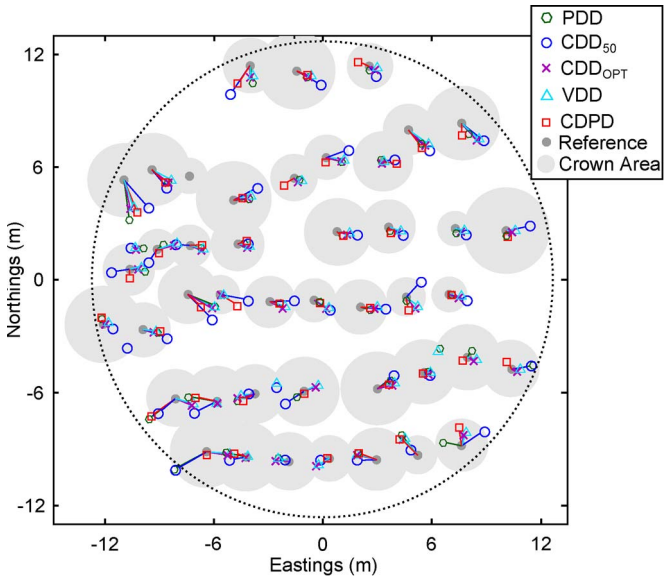

Fig. 5. Distribution of tree location errors over plot 6 using full-scale data within the five algorithms analyzed.

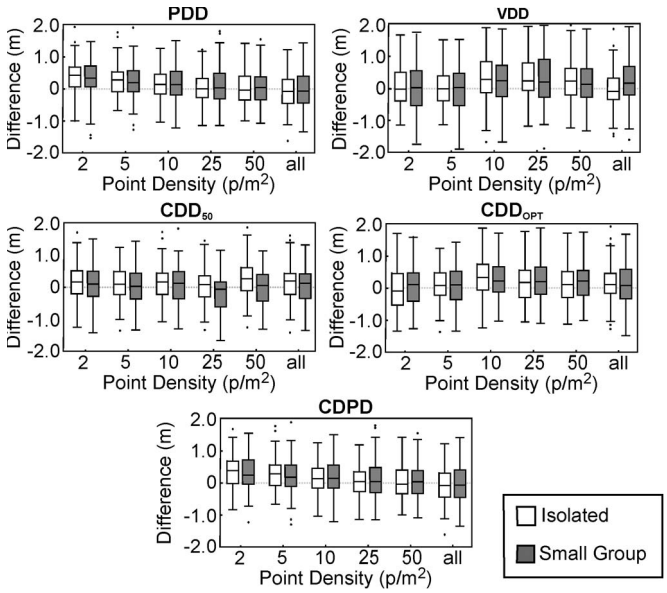

Fig. 6. Box plot (showing the 5th, 25th, 50th, 75th, and 95th quartiles) showing the difference between field and LiDAR measured crown widths of isolated trees and trees in small groups for each algorithm and at each density.

the individual algorithms used. This is indicated by the higher standard deviations found in all five algorithms, for instance, the VDD algorithm, which had a 0.71-m standard deviation when used with the 5-p/m^2 data set, had a 0.47-m standard deviation at full density.

C. Crown Width

The choice of algorithm had a significant effect on the accuracy of crown delineation at full density (see Fig. 6). The highest accuracy algorithm was CDPD at a density of 50 p/m^2, which had an RMSE of 0.38 m and a bias of 0.0 m. The PDD and CDD$_{\mathrm{opt}}$ algorithms also achieved low biases of 0.03 and −0.03 m at full density, respectively; however, the PDD algorithm had a significantly higher RMSE of 0.73 m. The VDD and CDD$_{50}$ algorithms tended to overestimate crown width at full density, indicated by the higher biases of 0.19 and 0.11 m.

The CDPD algorithm was the only algorithm where point density had a significant effect in reducing the RMSE of crown delineation. For the CDD$_{\mathrm{opt}}$, PDD, and CDPD algorithms, the overall biases decreased with increased point density (see Fig. 6). As these algorithms overestimate crown width at lower point densities, the decrease in bias can be correlated to the lower omission rates (i.e., from a crown being correctly split into two). In CDPD, CDD$_{\mathrm{opt}}$, PDD, and VDD algorithms, the bias of isolated trees tended to decrease with point density. In most algorithms, this resulted in the crown width being underestimated. The CDD$_{50}$ algorithm, which did not have a lower omission rate, showed no improvement or otherwise due to changes in point density.

V. Discussion

The results of this paper have shown that trees within a four-year-old Eucalyptus plantation can be more reliably detected and delineated from LiDAR data sets when very high density data is used. Similar to the earlier comparison study by Kaartinen *et al.* [32], the algorithm used had a significant effect on the rate of detection and accuracy of delineation when utilizing low-density point cloud data sets. At all point densities, the tree detection rate was higher than that found in prior studies using similar algorithms. Vauhkonen *et al.* [30] showed that the complexity of the forest had a significant influence on the detection results. Detection and delineation algorithms applied to plantation data sets have been shown to produce accurate and unbiased stem estimates [18], [43]. This is due to plantations consisting of even-age forests with regular planting patterns, with typically a low number of suppressed trees. Similarly, in this paper, the rate of omission for all algorithms was highest for suppressed trees that were part of a group for which there was only a small number. This negates the importance of selecting appropriate smoothing strategies in CHM-based algorithms for instance.

In contrast to the study of Roberts *et al.* [43], commission error tended to decrease with stem density. This again is due to the properties of the trees in the plantation. In our study, the structure of the trees was found for the most part to be poor, with 30% of the field-surveyed trees having at least one large ramicorn or fork, which presented as false maxima for individual tree detection. This issue mainly occurred in sparse stands, where these features tended to be more prominent. Often, these features were present at all point densities; therefore, there was no increase or otherwise in the commission rate with increasing point densities.

The primary advantage of using high point density data sets is to reduce omission rates, which was observed with most detection algorithms. Improvement with point density was seen at all densities and was found to be more significant than the algorithm used, which is contrary to findings of Kaartinen *et al.* [32] and Reitberger *et al.* [17]. One reason for this is that the

average number of strikes per tree was comparatively low at 2 and 5 p/m^2 in a study area consisting of young trees with a mean height of 7.6 m. Therefore, a similar increase in the pulse density represents a more significant increase in strikes per tree for this type of forest. This allows maxima and ridges of smaller trees to become more evident at higher densities.

The increase in tree detection rate in high-density point clouds can be attributed to the tree crowns being more accurately described. First, increasing the sampling density increases the likelihood of a treetop being observed in the data. Therefore, algorithms that rely on the accurate detection of maxima such as $\mathrm{CDD}_{\mathrm{opt}}$ are more likely to find trees in high-density data. The VDD algorithm, on the other hand, makes use of the increased definition of the crown boundaries within the raw data. The high point density allowed the voxel layer height to be decreased meaning that small trees growing in groups were observed as distinct segments in the upper voxel layers in which they occurred. The CDPD and PDD algorithms made use of all the available extra information in the point cloud. These algorithms had the greatest improvement in the omission rates between 5 p/m^2 and full density data (8% and 9%, respectively).

The achievable accuracy of crown delineation was not fully assessed by the algorithms used in this paper as the reference data consisted of only two measurements of crown width. Furthermore, the 1.3-m height threshold applied in all algorithms did not allow the trees to be fully segmented as they were unpruned and had crowns which extended to ground level. Although this was the case, the technique used to determine this metric in each algorithm was similar to the algorithm used in the field. Higher resolution data also allowed LiDAR crown widths of trees in groups to more closely match field-measured crown widths due to a reduction in the omission error.

Tree location accuracy was also improved by the use of full density data, as treetops had a higher likelihood of being observed within the data set. Similar to crown width, the reference data for the comparison were not of very high accuracy and a significant component of the error is a result of the error in the field measurements. Interestingly, the CDPD algorithm, which used cluster centers to represent tree location, conformed more closely to field-measured locations than other algorithms. This suggests that using within-cluster (or tree) information, such as with the CDPD algorithm or the algorithm in Reitberger *et al.* [17], has the potential to provide a more accurate estimate of stem location than the location of the tree top in this study area. This result is in contrast to [32], which found that an algorithm similar to CDPD resulted in tree locations with an RMSE of up to of 1.3 m in comparison to submeter RMSE values found in methods using the location of the highest point. More accurate reference information is required to fully test this theory.

It is important to note that all tree detection algorithms used in this paper require prior knowledge on the potential size and distribution of crown size within the stand. For instance, both the CHM and point cloud techniques require an initial estimate of crown width to achieve optimal results. In this paper, one plot was used to provide optimal tuning of each algorithm. This is an appropriate approach for plantation data sets where trees can be considered to have similar properties; however, more spatially adaptive tuning would be required for more variable stands. Several studies have presented algorithms, which aim to select an optimal kernel for use with the CHM by performing the same segmentation several times and examining the properties of the segmented trees, for example, in Ene *et al.* [44]. A similar technique for the optimal tuning of point cloud-based algorithms is also required; however, extracting the extra information from high-density point clouds adds extra computational burden and may preclude a similar approach. Future research is required to investigate methods that optimize tree detection algorithms based on the characteristics of the point cloud.

The results of this paper have confirmed that the tree detection algorithms analyzed are suitable for detecting and delineating individual trees within immature eucalyptus plantations at densities between 5 and 163 p/m^2. A density of 2 p/m^2, which is commonly collected for area-based analysis in the industry, does not allow accurate detection of trees within this forest type. This result suggests that 5 p/m^2 is the minimum density at which these algorithms can be applied for individual tree level analysis in this forest type. This result is, however, likely to vary within other forest types, particularly mixed species and multilayered forests.

Exploiting the on-demand nature of UAV surveys and collecting data at higher temporal frequencies will therefore allow plantation management decisions to be made with greater certainty. For instance, UAV data could be collected to remove subjectivity in determining the timing of pruning and thinning treatments. Further research is required to determine if estimates of other key inventory metrics such as the rate of canopy closure, the height of the trees, and the stem quality within young eucalyptus plantations can be made with the required accuracy from the data collected with UAVs.

VI. Conclusion

The unique characteristics of our LiDAR UAV platform allowed us to generate point clouds at very high densities (61–163 p/m^2). The short flight time of UAV platforms means that for the functional deployment of UAVs as a LiDAR system, sampling is likely to occur at the tree level, and as such, high accuracy of individual tree detection and delineation is essential. This paper has therefore compared several individual tree detection and delineation algorithms for use with high-density LiDAR data within a single four-year-old *Eucalyptus globulus* plantation.

The CDPD (k-means clustering) algorithm produced the best detection rate, correctly identifying 98% of the trees within the study area. Subsequently, this algorithm produced the lowest RMSE (0.43 m) and bias (0.01 m) in determining crown diameter. Although detection and delineation of trees using high-density data was achieved with acceptable accuracy for all algorithms, the choice of algorithm was shown to still be an important consideration. Furthermore, selecting appropriate data preparation parameters such as decreasing the CHM cell size to match the point density significantly improved tree detection and delineation outcomes.

This paper has also shown that within a four-year-old Eucalyptus plantation, point density significantly influences successful detection of individual trees from LiDAR point

clouds across a number of algorithms. The main improvement is a reduced rate of omission of up to 9% with a point density increase from 5 to 50 p/m^2. This represents a significant improvement considering the already high detection rates with low-density data [i.e., 85% of trees being detected with low density data (5 p/m^2)]. The improvement in tree detection also translates into a more accurate delineation of trees, with a reduction in the RMSEs of tree location and crown width shown in most algorithms used.

Although this paper used data collected from a UAV platform, we demonstrated that these data are similar to that of a traditional airborne LiDAR platform over our chosen forest type. The results of this paper therefore suggest that as high-density LiDAR data become increasingly available due to improved sensor designs on full-scale platforms and more flexible platforms, such as UAVs, the utilization of LiDAR derived individual tree inventories will become a more valuable option for the monitoring and management of eucalyptus plantations.

REFERENCES

[1] M. Wulder, C. Bater, and N. Coops, "The role of LiDAR in sustainable forest management," *Forest. Chron.*, vol. 84, no. 6, pp. 807–826, 2008.

[2] J. Hyyppä, M. Holopainen, and H. K. Olsson, "Laser scanning in forests," *Remote Sens.*, vol. 4, no. 10, pp. 2919–2922, Sep. 2012.

[3] R. Nelson, W. Krabill, and J. Tonelli, "Estimating forest biomass and volume using airborne laser data," *Remote Sens. Environ.*, vol. 24, no. 2, pp. 247–267, Mar. 1988.

[4] P. Packalén and M. Maltamo, "The k-MSN method for the prediction of species-specific stand attributes using airborne laser scanning and aerial photographs," *Remote Sens. Environ.*, vol. 109, no. 3, pp. 328–341, Aug. 2007.

[5] E. Næsset, "Predicting forest stand characteristics with airborne scanning laser using a practical two-stage procedure and field data," *Remote Sens. Environ.*, vol. 80, no. 1, pp. 88–99, Apr. 2002.

[6] J. Holmgren, "Prediction of tree height, basal area and stem volume in forest stands using airborne laser scanning," *Scand. J. Forest Res.*, vol. 19, no. 6, pp. 543–553, Dec. 2004.

[7] A. T. Hudak, N. L. Crookston, J. S. Evans, D. E. Hall, and M. J. Falkowski, "Nearest neighbor imputation of species-level, plot-scale forest structure attributes from LiDAR data," *Remote Sens. Environ.*, vol. 112, no. 5, pp. 2232–2245, May 2008.

[8] M. Wulder *et al.*, "LiDAR sampling for large-area forest characterization: A review," *Remote Sens. Environ.*, vol. 121, pp. 196–209, Jun. 2012.

[9] J. Hyyppä and M. Inkinen, "Detection and estimating attributes for single trees using laser scanner," *Photogramm. J. Finland*, vol. 16, pp. 27–42, 1999.

[10] A. Jaakkola *et al.*, "A low-cost multi-sensoral mobile mapping system and its feasibility for tree measurements," *ISPRS J. Photogramm. Remote Sens.*, vol. 65, no. 6, pp. 514–522, Nov. 2010.

[11] L. Wallace, A. Lucieer, C. Watson, and D. Turner, "Development of a UAV-LiDAR system with application to forest inventory," *Remote Sens.*, vol. 4, no. 6, pp. 1519–1543, May 2012.

[12] L. Wallace, A. Lucieer, and C. Watson, "Assessing the feasibility of UAV-based LiDAR for high resolution forest change detection," in *Proc. ISPRS, Int. Archives Photogramm., Remote Sens. Spatial Inf. Sci.*, 2012, vol. 38-B7, pp. 499–504.

[13] M. Maltamo *et al.*, "Identifying and quantifying structural characteristics of heterogeneous boreal forests using laser scanner data," *Forest Ecol. Manage.*, vol. 216, no. 1–3, pp. 41–50, Sep. 2005.

[14] B. Koch, U. Heyder, and H. Weinacker, "Detection of individual tree crowns in airborne LiDAR data," *Photogramm. Eng. Remote Sens.*, vol. 72, no. 4, pp. 357–363, Apr. 2006.

[15] Y. Wang, H. Weinacker, B. Koch, and K. Sterenczak, "LiDAR point cloud based fully automatic 3D single tree modelling in forest and evaluations of the procedure," in *Proc. Int. Archives Photogramm., Remote Sens. Spatial Inf. Sci.*, 2008, vol. 37, pp. 45–52.

[16] C. Alexander, "Delineating tree crowns from airborne laser scanning point cloud data using Delaunay triangulation," *Int. J. Remote Sens.*, vol. 30, no. 14, pp. 3843–3848, Jul. 2009.

[17] J. Reitberger, C. Schnörr, P. Krzystek, and U. Stilla, "3D segmentation of single trees exploiting full waveform LiDAR data," *ISPRS J. Photogramm. Remote Sens.*, vol. 64, no. 6, pp. 561–574, Nov. 2009.

[18] J. Vauhkonen, L. Mehtätalo, and P. Packalén, "Combining tree height samples produced by airborne laser scanning and stand management records to estimate plot volume in Eucalyptus plantations," *Can. J. Forest Res.*, vol. 41, no. 8, pp. 1649–1658, Aug. 2011.

[19] T. Brandtberg, "Detection and analysis of individual leaf-off tree crowns in small footprint, high sampling density LiDAR data from the eastern deciduous forest in North America," *Remote Sens. Environ.*, vol. 85, no. 3, pp. 290–303, May 2003.

[20] F. Morsdorf, E. Meier, B. Allgöwer, and D. Nuesch, "Clustering in airborne laser scanning raw data for segmentation of single trees," in *Proc. Int. Archives Photogramm, Remote Sens. Spatial Inf. Sci.*, 2003, vol. 34 Part 3, pp. 27–33.

[21] W. Li and Q. Guo, "A new method for segmenting individual trees from the LiDAR point cloud," *Photogramm. Eng. Remote Sens.*, vol. 78, no. 1, pp. 75–84, Jan. 2012.

[22] T. Lahivaara *et al.*, "Bayesian approach to tree detection with airborne laser scanning," in *Proc. IEEE Int. Geosci. Remote Sens. Symp.*, Munich, Germany, Jul. 2012, pp. 1641–1644.

[23] X. Yu, J. Hyyppä, M. Vastaranta, M. Holopainen, and R. Viitala, "Predicting individual tree attributes from airborne laser point clouds based on the random forests technique," *ISPRS J. Photogramm. Remote Sens.*, vol. 66, no. 1, pp. 28–37, Jan. 2011.

[24] N. R. Vaughn, L. M. Moskal, and E. C. Turnblom, "Tree species detection accuracies using discrete point LiDAR and airborne waveform LiDAR," *Remote Sens.*, vol. 4, no. 2, pp. 377–403, Feb. 2012.

[25] J. Peuhkurinen, L. Mehtätalo, and M. Maltamo, "Comparing individual tree detection and the area-based statistical approach for the retrieval of forest stand characteristics using airborne laser scanning in Scots pine stands," *Can. J. Forest Res.*, vol. 41, no. 3, pp. 583–598, Mar. 2011.

[26] M. Vastaranta *et al.*, "Effects of individual tree detection error sources on forest management planning calculations," *Remote Sens.*, vol. 3, no. 8, pp. 1614–1626, Aug. 2011.

[27] J. Pitkänen, M. Maltamo, J. Hyyppä, and X. Yu, "Adaptive methods for individual tree detection on airborne laser based canopy height model," in *Proc. ISPRS Workshop Laser-Scanners Forest Landscape Assess.*, Freiburg, Germany, 2004, pp. 187–191.

[28] J. N. Heinzel, H. Weinacker, and B. Koch, "Prior-knowledge-based single-tree extraction," *Int. J. Remote Sens.*, vol. 32, no. 17, pp. 4999–5020, Sep. 2011.

[29] J. Hyyppä *et al.*, "HIGH-SCAN: The first European-wide attempt to derive single-tree information from laser scanner data," *Photogramm. J. Finland*, vol. 17, no. 2, pp. 58–68, 2001.

[30] J. Vauhkonen *et al.*, "Comparative testing of single-tree detection algorithms under different types of forest," *Forestry*, vol. 85, no. 1, pp. 27–40, Jan. 2011.

[31] C. Edson and M. G. Wing, "Airborne Light Detection and Ranging (LiDAR) for individual tree stem location, height, biomass measurements," *Remote Sens.*, vol. 3, no. 11, pp. 2494–2528, Nov. 2011.

[32] H. Kaartinen *et al.*, "An international comparison of individual tree detection and extraction using airborne laser scanning," *Remote Sens.*, vol. 4, no. 4, pp. 950–974, Mar. 2012.

[33] M. K. Jakubowski, Q. Guo, and M. Kelly, "Tradeoffs between LiDAR pulse density and forest measurement accuracy," *Remote Sens. Environ.*, vol. 130, pp. 245–253, Mar. 2013.

[34] J. Vauhkonen, T. Tokola, M. Maltamo, and P. Packalén, "Effects of pulse density on predicting characteristics of individual trees of Scandinavian commercial species using alpha shape metrics based on airborne laser scanning data," *Can. J. Remote Sens.*, vol. 34, no. S2, pp. S441–S459, Nov. 2008.

[35] G. Raber *et al.*, "Impact of LiDAR nominal post-spacing on DEM accuracy and flood zone delineation," *Photogramm. Eng. Remote Sens.*, vol. 73, no. 7, pp. 793–804, Jul. 2007.

[36] X. Meng, N. Currit, and K. Zhao, "Ground filtering algorithms for airborne LiDAR data: A review of critical issues," *Remote Sens.*, vol. 2, no. 3, pp. 833–860, Mar. 2010.

[37] P. Axelsson, "Processing of laser scanner data—Algorithms and applications," *ISPRS J. Photogramm. Remote Sens.*, vol. 54, no. 2/3, pp. 138–147, Jul. 1999.

[38] J. R. Ben-Arie, G. J. Hay, R. P. Powers, G. Castilla, and B. St-Onge, "Development of a pit filling algorithm for LiDAR canopy height models," *Comput. Geosci.*, vol. 35, no. 9, pp. 1940–1949, Sep. 2009.

[39] A. Persson, J. Holmgren, and U. Soderman, "Detecting and measuring individual trees using an airborne laser scanner," *Photogramm. Eng. Remote Sens.*, vol. 68, no. 9, pp. 925–932, Sep. 2002.

[40] M. Maltamo *et al.*, "Predicting tree attributes and quality characteristics of scots pine using airborne laser scanning data," *Silva Fennica*, vol. 43, no. 3, pp. 507–521, 2009.
[41] S. Gupta, H. Weinacker, and B. Koch, "Comparative analysis of clustering-based approaches for 3-D single tree detection using airborne fullwave LiDAR data," *Remote Sens.*, vol. 2, no. 4, pp. 968–989, Apr. 2010.
[42] S. C. Popescu, "Estimating biomass of individual pine trees using airborne LiDAR," *Biomass Bioenergy*, vol. 31, no. 9, pp. 646–655, Sep. 2007.
[43] S. D. Roberts *et al.*, "Estimating individual tree leaf area in loblolly pine plantations using LiDAR-derived measurements of height and crown dimensions," *Forest Ecol. Manage.*, vol. 213, no. 1–3, pp. 54–70, Jul. 2005.
[44] L. Ene, E. Næsset, and T. Gobakken, "Single tree detection in heterogeneous boreal forests using airborne laser scanning and area-based stem number estimates," *Int. J. Remote Sens.*, vol. 33, no. 16, pp. 5171–5193, Aug. 2012.

Luke Wallace received the Bachelors of Spatial Science degree (with honors) from the University of Tasmania, Hobart, Australia, in 2005, where he is currently working toward the Ph.D. degree in the School of Land and Food.

His current research interests focus on the use of Bayesian estimation for determination of unmanned aerial vehicle position and orientation using vision and microelectromechanical system-based devices for direct georeferencing of imagery and LiDAR data with application to forestry.

Arko Lucieer received the M.Sc. degree in physical geography with a specialization in hyperspectral remote sensing from Utrecht University, Utrecht, The Netherlands, in 2000 and the Ph.D. degree from the International Institute for Geo-Information Science and Earth Observation (ITC), Enschede, The Netherlands, and Utrecht University in 2004. His Ph.D. research focused on image segmentation and visualization of uncertainty in satellite imagery.

In 2004, he was a Lecturer with the School of Land and Food, University of Tasmania, Hobart, Australia, where he has been a Senior Lecturer in remote sensing and geographic information system since 2010. The focus of his research is on texture measures, image segmentation and fuzzy classification, GEOBIA, and change detection techniques. In 2010, he founded a research group focusing on the use of unmanned aircraft systems and miniature sensors for environmental remote sensing and aerial surveys.

Christopher S. Watson received the Ph.D. degree from the University of Tasmania, Hobart, Australia, in 2005, with his research focusing on satellite altimeter validation using GPS buoy technology.

He has a background in positioning and high-accuracy measurement and is a Senior Lecturer in geodesy with the School of Land and Food, University of Tasmania, Hobart, Australia. His current research interests have an emphasis on "environmental geodesy," i.e., the use of space and airborne geodetic tools such as GNSS, satellite and airborne altimetry, and space gravity applied to global climate change and sea-level studies, crustal dynamics, and surface expression of mass loads. He has a particular focus on the detection and mitigation of systematic error sources across a range of measurement platforms spanning satellite to unmanned aerial systems.